


# Assessment of aliphatic poly(ester-carbonate-urea-urethane)s potential as materials for biomedical application

Joanna Mystkowska<sup>1</sup> · Magdalena Mazurek-Budzyńska<sup>2</sup>  · Ewelina Piktel<sup>3</sup> · Katarzyna Niemirowicz<sup>3</sup> · Wojciech Karalus<sup>1</sup> · Piotr Deptuła<sup>1,3</sup> · Katarzyna Pogoda<sup>4</sup> · Dawid Łysik<sup>1</sup> · Jan Ryszard Dąbrowski<sup>1</sup> · Gabriel Rokicki<sup>2</sup> · Robert Bucki<sup>3</sup>

Received: 21 April 2017 / Accepted: 31 July 2017 / Published online: 17 August 2017  
© The Author(s) 2017. This article is an open access publication

**Abstract** Selected mechanical and biological properties of biodegradable elastomeric poly(ester-carbonate-urea-urethane)s (PECUUs) point towards their potential to be applied as scaffolds in tissue engineering. Here we explore their medical applicability taking into account their hemocompatibility and cytotoxicity. The influence of the ester monomer (derivatives of adipic and succinic acids), as well as diisocyanate type (IPDI and HDI) on the investigated PECUUs properties is presented. The presence of aliphatic diisocyanates, cyclic IPDI or linear HDI, governs the adhesion of *Candida* cells to these polymers offering the possibility to control the biofilm formation on their surface. In comparison to the linear form, cyclic diisocyanates with pentamethylene succinate or adipate fragments had two to three times lower biofilm mass formation on their surface. Reduced hemoglobin release from red blood cells observed during incubation of tested polymers with human erythrocytes suspension indicates their potential biocompatibility with human

tissues. PECUUs were also able to support the growth of human keratinocytes HaCaT on their surface when coated with collagen. In effect, IPDI derivatives might possess a high potential for use in biomedical applications.

**Keywords** Poly(ester-carbonate-urea-urethane)s · Elastomer · *Candida* biofilm · Biocompatible polymers · Mechanical properties

## Introduction

Because of the combination of excellent biocompatibility and mechanical properties such as flexural endurance, high strength, and high abrasion resistance, polyurethanes (PURs) are one of the most frequently used plastics in medical applications [1–7]. Specific properties of polyurethanes depend on the chemical composition, which as a result of the synthesis method, can be widely varied. PURs have a structure of a multiblock copolymer, consisting of hard and soft segment domains. Hard segments are derivatives of diisocyanates and chain extenders. Soft segments are introduced with the oligomerol, among which the most common are oligoesters [8–10], oligoetherols [11–13], and oligocarbonate diols [14]. Poly(ester-urethane)s (PEUs) undergo significant hydrolytic degradation *in vivo*; therefore, they are unsuitable for long-term implants [15, 16]. Furthermore, due to the presence of carboxylic groups in the main chain of the PEUs, hydrolytic degradation leads to local decrease of pH and causing a strong inflammatory response. Therefore, much attention has been given to exploring an alternative material with improved biocompatibility while maintaining the beneficial mechanical properties. A relatively new generation of polyurethanes used in medical devices are based on poly(carbonate-urethane)s (PCUs). According to *in vitro* and early *in vivo* studies,

✉ Joanna Mystkowska  
j.mystkowska@pb.edu.pl

✉ Magdalena Mazurek-Budzyńska  
mmazurek@ch.pw.edu.pl

<sup>1</sup> Faculty of Mechanical Engineering, Department of Materials and Biomedical Engineering, Białystok University of Technology, Wiejska 45C, 15-351 Białystok, Poland

<sup>2</sup> Department of Chemistry, Chair of Polymer Chemistry and Technology, Warsaw University of Technology, Noakowskiego 3, 00-664 Warsaw, Poland

<sup>3</sup> Department of Microbiological and Nanobiomedical Engineering, Medical University of Białystok, Mickiewicza 2C, 15-222 Białystok, Poland

<sup>4</sup> Institute of Nuclear Physics, Polish Academy of Sciences, Radzikowskiego 152, 31-342 Cracow, Poland

PCUs exhibit improved resistance to hydrolytic degradation and in vivo stress cracking compared to oligoester based medical grade polyurethanes [17–24]. Furthermore, according to the mechanism of hydrolytic degradation of PCUs [25], a decrease of pH is not observed, which leads to a much lower inflammation of the surrounding tissues. Therefore, PCUs have been intensively investigated as suitable materials for medical applications such as the artificial heart, pacemaker lead insulation, and meniscus or spine implants [26–31].

Furthermore, there is a critical need for the development of new biocompatible materials to limit the growing number of life-threatening infections associated with the use of medical devices [32]. The formation of pathogenic biofilms, especially by *Candida* species, requires initial surface adhesion and is one of the virulence factors that facilitate the colonization of medical devices [33, 34]. Chronic and recurrent fungal infections, as well as bloodstream invasive candidiasis are a consequence of pathogenic biofilm formation [34, 35]. Therefore, the restrictions of biofilm growth via inhibition of metabolic activity, pathogen communication or selective eradication of cells embedded in the biofilm matrix are important challenges facing modern medicine. A promising strategy to address these issues is the creation of materials that possess surface properties, which inhibit biofilm formation.

In this study we have combined properties of PEUs and PCUs by preparing poly(ester-carbonate-urea-urethane) (PECUU) elastomers with the aim to explore their potential as building blocks for polymeric scaffolds used in regenerative medicine. Mechanical and thermal properties of PECUUs, water uptake, and pH of water solution after sample immersion were also examined. In addition the biological response towards the scaffolds in terms of their hemocompatibility, direct cytotoxicity, and resistance to biofilm formation was studied.

## Experimental section

### Materials

Poly(ester-carbonate-urea-urethane)s were obtained by the precursor method according to the procedure previously published [36]. In the first step urethane prepolymer functionalized with isocyanate groups were obtained by the reaction of oligo(ester-carbonate) diol with an 3-M excess of diisocyanate (IPDI or HDI). Then the reaction mixture was poured into the PTFE open cylindrical mold of the diameter of 10 cm and placed in the climate chamber, in which the process of chain extending of urethane prepolymer was performed under controlled conditions of humidity and temperature [36]. Oligo(alkylene succinate-co-carbonate) diols (PSC) and

oligo(pentamethylene adipate-co-carbonate)s (PAC) were synthesized based on bis(methyl carbonate)s and dimethyl succinate or dimethyl adipate in the two step process described in details in one of our previous work [36]. The protocol used for alkylene bis(methylcarbonate) synthesis from 1,4-butanediol or 1,5-pentanediol and dimethyl carbonate is reported elsewhere [37]. As a catalyst,  $\text{Ti}(\text{O}i\text{Bu})_4$  (0.01% mol/mol of diol) was used.

### Characterization technique

$^1\text{H}$  NMR spectra were recorded on a Varian VXR 400 MHz spectrometer using tetramethylsilane as an internal standard, and  $\text{CDCl}_3$  or  $\text{DMSO-d}_6$  as a solvent. DSC studies were carried out using a TA Instruments DSC Discovery apparatus. The measurements were conducted in three cycles (heat-cool-heat), in a temperature range from  $-80$  to  $250$  °C with a heating and cooling rate of  $10$  °C·min $^{-1}$ . Three samples of each polymer were analyzed. Values of  $T_g$  were obtained based on point of inflection of DSC curve. Density was determined using helium pycnometer (AccuPyc, Micromeritics) equipped with  $1$  cm $^3$  chamber. Water sorption was evaluated by measuring the percentage weight increase of a dry polymer sample after immersion for 24 h in distilled water at  $37$  °C. To check the changes in pH of the water, polymer samples were immersed in distilled water for 14 and 28 days at  $37$  °C. Values of pH were carried out by means of suitable measuring electrodes cooperating with the multifunctional SevenMultimeter (Mettler Toledo, Switzerland). Ratings of pH were determined using a Clarytrode 120 electrode. Hardness measurements of polyurethane films were performed using a Shore hardness tester (A-scale). Friction tests were conducted using the T-11 type pin-on-disc tester under dry environment. A general view of the research station and the friction pair is shown elsewhere [38]. The friction pair was composed of a pin (polymer sample) with a diameter of 3 mm and a counter sample was a disc (corundum ceramics) with diameter of 25.4 mm and  $R_a = 2.2$  μm. On the basis of the performed initial research, the following parameters were adopted for the tribological tests: friction velocity,  $v = 0.1$  m/s; friction radius  $r = 8$  mm; counter sample (disc) rotational velocity  $n = 120$  rpm; load force applied on the sample  $F = 15$  N; time of friction in a single test  $t = 0.5$  h. The mass wear of the friction node was calculated after process. Measurements of tensile strength were performed using Instron 5566 machine with a constant stretching rate of 100 mm/min. The samples were dog-bone shaped with 30 mm length, 5 mm width, and 1 mm thickness of the measuring segment. For the data processing Bluehill software was used. The obtained results were statistically processed using the STATISTICA software package, StatSoft Company. All the observed characteristics are the mean values obtained

from six tests performed under the same measurement conditions at ambient temperature. Results are displayed as the mean  $\pm$  standard deviation. The results were considered statistically significant at  $p < 0.05$ . In order to determine the level of significance, the following  $p$ -values were used:  $*p < 0.05$ ,  $**p < 0.01$ ,  $***p < 0.001$  vs. distilled water. **Local mechanical properties** of the PCEUUs were assessed using NanoWizard 4 BioScience atomic force microscope (JPK Instruments, Germany). Quantitative Imaging mode (QI) was used to register so-called force-curves at every pixel of the image. Scan size was adjusted to be  $10 \mu\text{m} \times 10 \mu\text{m}$  with the resolution of  $256 \times 256$  pixels. Conical-shaped AFM cantilevers with nominal spring constant equal  $3.4 \text{ N/m}$  and nominal tip radius equal  $8 \text{ nm}$  (MikroMasch, Bulgaria) were used as a probe. The force-curves were collected with constant velocity equal  $300 \mu\text{m/s}$ . Because of the observed attractive forces acting in the region where the cantilever-sample contact was made, Young's modulus calculations based on Hertz contact mechanics were unreasoned. Through this limitation the slope of the force curve while z-piezo extension was used as a quantity describing local sample stiffness. During z-piezo retraction the pull-off force which prevents cantilever-sample separation was observed and used to calculate the adhesion force acting between the cantilever tip and sample surface (Fig. 1).

The cantilever spring constants were calibrated before each measurement based on the thermal tune method using a built-in algorithm and the z-piezo range set to  $3.5 \mu\text{m}$ . All of the measurements were performed at room temperature (RT). The data were analyzed using JPK SPM data processing software.

### Biofilm formation

Clinical isolates of *Candida tropicalis* (obtained from a patient with a skin infection) were cultured on SDA agar to mid-log phase at  $37 \text{ }^\circ\text{C}$ . Then, yeast cells were re-suspended in LB medium and brought to  $\text{OD}_{600} = 0.1$ . Tested polymeric surface were placed into 24-wells in  $1 \text{ mL}$  LB medium containing *Candida* suspension ( $500 \mu\text{L}$ ). *Candida* biofilms were grown for  $48 \text{ h}$  at  $37 \text{ }^\circ\text{C}$  in the presence of tested polymers.

### Biomass quantification

The surface of each tested polymer was thoroughly rinsed with deionized water to remove planktonic cells. The total biomass was evaluated using crystal violet (CV) staining methods. After washing the unlinked dye,  $100 \mu\text{L}$  of ethanol was added. Then,  $100 \mu\text{L}$  of solubilized CV samples were transferred to clear 96-well plates and the optical density (OD) was determined spectrophotometrically at a wavelength of  $570 \text{ nm}$ . These OD values were considered as an index of

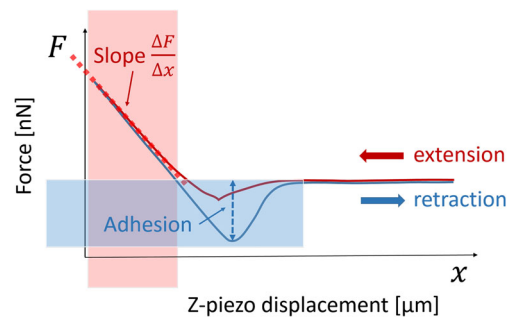


**Fig. 1** Demonstration of force curves used to determine stiffness and adhesion by atomic force microscopy (AFM)

fungal cells in biofilm matrix adhering to the surface. Results were normalized to biofilm growth on a polystyrene surface.

### Investigation of biofilms topography by atomic force microscopy

Additionally, the morphology of *Candida* biofilms was investigated using NanoWizard 4 BioScience atomic force microscope (JPK Instruments, Germany). Because of the expected low stiffness of fungal cells compared to tested polymers, ORC8 (Bruker) four-sided pyramid cantilevers with nominal spring constant equal  $0.38 \text{ N/m}$  were employed. Quantitative Imaging mode was used for height maps collection. Scan size was set to  $20 \mu\text{m} \times 20 \mu\text{m}$  and  $256 \times 256$  pixels spatial resolution. All the measurements were carried out on living biofilm immersed in PBS at room temperature. The force-curves were collected with constant velocity equal  $300 \mu\text{m/s}$  and the z-piezo range set to  $15 \mu\text{m}$ . Spring constants of the cantilevers were calibrated based on thermal tune method priori to each measurement. The results are presented as a 3D height maps.

### Evaluation of hemocompatibility

A hemolysis assay was performed in order to assess the hemocompatibility of tested polymers. For this purpose, a square fragments of polymers with comparable surface area (weight approx.  $5 \text{ mg}$ ) were incubated in phosphate-buffered saline (PBS) supplemented with glucose and containing suspended human red blood cells (RBCs) and hematocrit  $\sim 5\%$  (total volume of sample was  $200 \mu\text{L}$ ). Incubation was carried out at  $37 \text{ }^\circ\text{C}$  for up to  $24 \text{ h}$ . At the indicated time points ( $1, 6, 18,$  and  $24 \text{ h}$ ),  $40 \mu\text{L}$  of RBC suspensions was centrifuged ( $2500 \text{ g}$ ,  $10 \text{ min}$ ) and the relative hemoglobin concentration in supernatants was monitored by measuring optical absorbance at  $540 \text{ nm}$ .  $100\%$  hemolysis was taken from samples in which  $1\%$  Triton X-100 was added to disrupt all the cell membrane and compared to the values obtained for negative control (RBCs suspension without polymers).

## Evaluation of direct cytotoxicity

Additionally, to evaluate the cytotoxicity of tested materials, polymers were transferred to 12-well cell culture treated plates and pre-coated with collagen I (0.1 mg/mL, 2 h incubation). Then, on their surface a suspension of HaCaT cells (immortalized, human keratinocyte cell line) at a density of  $1.2 \times 10^4$  cells/well was seeded and cultured in DMEM medium supplemented with 10% fetal bovine serum, 50 U/mL penicillin, and 50 mg/mL streptomycin at 37 °C in a 5% CO<sub>2</sub> incubator for up to 72 h. At the indicated time points (24, 48, and 72 h) optical images were collected in order to count the number of cells attached to the polymer surface. The number of cells at the surface of materials was compared to the number of cells growing on the surface of the cell culture plates.

For fluorescence-based assessment of morphology of the cells, HaCaT cells were seeded on the collagen-coated polymers at the density of  $4 \times 10^4$  cells per each well of 12-well cell culture treated plate and cultured for 24 h at 37 °C in a 5% CO<sub>2</sub> incubator. After incubation, polymers were transferred to 96-well plate and cells attached to the surface of polymers were stained with Hoechst 33,342 and Alexa Fluor® 488 Phalloidin in order to visualize the cell nuclei and actin cytoskeleton, respectively. For this purpose, polymers were washed twice with pre-warmed PBS and fixed in 3.7% formaldehyde solution in PBS for 15 min at room RT. After incubation of cells with Triton X-100 (0.1% in PBS, 5 min, RT), cells were stained sequentially with Hoechst 33,342 (0.1 µg/mL for 5 min at RT) and Alexa Fluor® 488 Phalloidin (1:1000 dilution; 30 min at RT). Stained samples were visualized using fluorescent microscope.

## Results

### Characteristics of oligo(ester-co-carbonate) diols

Based on <sup>1</sup>H NMR spectral analysis, the amount of carbonate units, as well as the molecular weight of the obtained oligo(ester-co-carbonate)s were estimated and are presented in Table 1. *TSCD* means oligo(tetramethylene succinate-co-carbonate) diol, *PSCD* means oligo(pentamethylene succinate-co-carbonate) diol, and *PACD* means oligo(pentamethylene adipate-co-carbonate) diol. Relevant structures of **TSCD**, **PSCD**, and **PACD** are presented in Scheme 1 a).

### Characteristics of poly(ester-carbonate-urea-urethane)s

The thermal properties of poly(ester-carbonate-urea-urethane)s were investigated. The results of differential scanning calorimetry (Table 2) show that all of the tested polymers exhibit low glass transition temperatures ( $T_g$ ), in the range between -46 and -33 °C. Depending on the diisocyanate

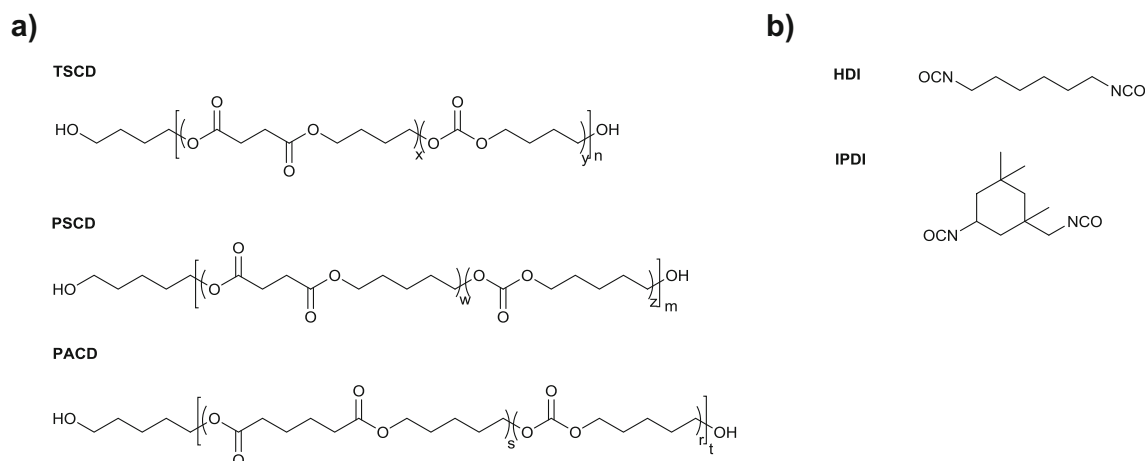
**Table 1** Characteristics of oligo(ester-co-carbonate) diols

| Run | Sample  | Content of carbonate units (mol.%) | $M_n$ (g·mol <sup>-1</sup> ) |
|-----|---------|------------------------------------|------------------------------|
| 1   | TSCD-53 | 53                                 | 2800                         |
| 2   | PSCD-36 | 36                                 | 1700                         |
| 3   | PSCD-44 | 44                                 | 3000                         |
| 4   | PACD-36 | 36                                 | 2300                         |
| 5   | PACD-51 | 51                                 | 2400                         |

used, slight differences in thermal properties were also observed. Comparison of **TSCD-53-HDI** and **TSCD-53-IPDI** (Table 2, runs 1 and 2) reveals increased  $T_g$  when IPDI is used. This is the result of the notably stiffer IPDI cyclic structure in contrast to the long and flexible chain of HDI (Scheme 1 b). Additionally, the length of hydrocarbon chain introduced with the ester monomer influences the thermal properties of investigated materials (Table 2, runs 3 and 5). The addition of two methylene groups in the polymer chain repeating unit via adipic acid derivative decreases the  $T_g$  from -42 °C for **PSCD-36-HDI** to -53 °C for **PACD-36-HDI**. Subsequently, due to the longer hydrocarbon chain, the  $T_m$  increases from approximately 58 to 68 °C. In the DSC thermodiagrams the exothermic peaks above 175 °C ( $T_d$ ), related most probably to the dissociation of the hydrogen bonds, were also observed. It should be noted that during second heating, melting points were not observed for tested polymers.

Results of tensile tests indicate that all of the synthesized polyurethanes were elastomers, with tensile strengths ( $\sigma$ ) ranging from  $20 \pm 1$  to  $58 \pm 8$  MPa and elongations at break ( $\epsilon$ ) in the range of  $500 \pm 76$  to  $750 \pm 50\%$  (Table 3). Hardness tests using Shore'a durometer indicate that among the tested polymer groups, materials based on HDI were characterized by increased hardness compared to IPDI-based polymers. As expected, PUR based on TSCD had the highest hardness (Table 3). This is a result of its highly packed and stiff structure due to the usage of 1,4-butanediol (short hydrocarbon chain with even number of methylene group), HDI, and high content (>50 mol%) of carbonate units.

Local mechanical properties of the polymeric surfaces were quantified using atomic force microscopy. This technique allows for the measurements at the micro- and nanoscale, which is relevant for single cell-surface interactions. The height maps presented in Figs. 2A-F reflect surface topographies. The spatial distributions of stiffness and adhesion forces are presented in Figs. 2G-S, where local inhomogeneities of both quantities can be observed. Local stiffness (N/m), which is a measure of sample rigidity, differs between the studied surfaces and is the lowest for **PSCD-36-HDI** and **PACD-51-IPDI** and the highest for **PSCD-44-IPDI** and **TSCD-53-IPDI**, respectively (Fig. 2G-L). Adhesion forces acting between the tip and sample surface are the highest for **PSCD-**



**Scheme 1** Structures of oligo(ester-co-carbonate) diols (**a**) and diisocyanates (**b**) used for the synthesis of PECUUs

**36-HDI** and the lowest for **PACD-51-IPDI**. Mean stiffness values and their standard deviations are presented in (Fig. 2M-S, Table 4).

### Tribological studies

During tribological tests, the coefficient of friction (Fig. 3A) for polymer-corundum cooperating pair was examined. Additionally, the mass wear (Fig. 3B) of polymers after friction process was calculated. In Fig. 3A results of friction coefficients, expressed as mean from 30 min of friction, are presented.

The lowest values of the coefficient of friction ( $\mu \sim 0.75$ ) was obtained for the friction pair with **PSCD-36-HDI** and **TSCD-53-HDI** polymers used as pins (Fig. 3A). These polymers also had the highest wear mass of the tested materials, as well as the highest hardness (Table 3). For materials with lower hardness and higher elasticity, an elevated coefficient of friction was observed. This suggests that wear particles of polymers were attached to the polymer surface and participated in generating friction. This was confirmed by mass wear (Fig. 3B), which was the lowest for the more elastic polymers ( $m_w = 0.0024$  g for **PSCD-44-IPDI** and  $m_w = 0.0017$  g for

**PACD-51-IPDI**). The mass wear for the other polymers was in the range of 0.004 to 0.009 g. These results are similar to those obtained in previously published work, where poly(carbonate-urethane)s composites embedded with ultrahigh molecular weight polyethylene fibers were evaluated [39]. However, in our current work, the friction process was performed by simulating loading for a total of five million gait cycles, corresponding to approximately 5 years of service in vivo. In previous work that mimicked the natural synovial joint conditions, the gravimetric wear of poly(carbonate-urethane) materials was in the range of 10 to 12.5 mg per million cycles [31].

### Water sorption ( $w_s$ )

Water sorption was evaluated by measuring the percentage weight increase of dry polymer sample after immersion in distilled water for 24 h (Fig. 4A). Because of the content of carbonate linkages all of the samples demonstrated low water sorption (around 2%). Previous work from Wang et al. [11] showed that poly(ether-carbonate-urethane-urea)s had higher values of water sorption. As indicated in Fig. 4A, TSCD samples had the highest water sorption of the tested materials

**Table 2** Results of poly(ester-carbonate-urea-urethane)s thermal analysis

| Run | Sample       | $T_g$<br>(°C)   | $T_m$<br>(°C) | $\Delta H_m$<br>(J/g) | $T_d$<br>(°C) | $\Delta H_d$<br>(J/g) |
|-----|--------------|-----------------|---------------|-----------------------|---------------|-----------------------|
| 1   | TSCD-53-HDI  | $-37.7 \pm 0.1$ | $48 \pm 1$    | $3.6 \pm 0.3$         | $191 \pm 2$   | $10.1 \pm 1.4$        |
| 2   | TSCD-53-IPDI | $-33.2 \pm 0.1$ | $50 \pm 1$    | $5.4 \pm 0.5$         | $183 \pm 2$   | $8.9 \pm 1.2$         |
| 3   | PSCD-36-HDI  | $-42.6 \pm 0.1$ | $58 \pm 1$    | $4.9 \pm 0.5$         | $177 \pm 1$   | $6.7 \pm 0.9$         |
| 4   | PSCD-44-IPDI | $-37.7 \pm 0.1$ | a)            | a)                    | $199 \pm 2$   | $10.8 \pm 1.5$        |
| 5   | PACD-36-HDI  | $-53.1 \pm 0.1$ | $68 \pm 2$    | $2.2 \pm 0.2$         | $178 \pm 1$   | $7.2 \pm 1.0$         |
| 6   | PACD-51-IPDI | $-46.0 \pm 0.1$ | a)            | a)                    | $203 \pm 2$   | $11.9 \pm 1.6$        |

a) The crystalline phase of the sample was not detected

**Table 3** Density and mechanical properties of poly(ester-carbonate-urea-urethane)s

| Sample       | Density,<br>$\rho$ (g/cm <sup>3</sup> ) | Tensile strength,<br>$\sigma$ (MPa) | Elongation at break,<br>$\varepsilon$ (%) | Hardness,<br>$SH$ (°S) |
|--------------|---|-------------------------------------|---|------------------------|
| TSCD-53-HDI  | 1.23 ± 0.0007                           | 58 ± 8                              | 500 ± 76                                  | 80.8 ± 1.3             |
| TSCD-53-IPDI | 1.21 ± 0.0030                           | nd                                  | nd  | 75.0 ± 0.9             |
| PSCD-36-HDI  | 1.17 ± 0.0005                           | 26 ± 1                              | 575 ± 26                                  | 80.0 ± 0.9             |
| PSCD-44-IPDI | 1.16 ± 0.0005                           | 20 ± 1                              | 750 ± 50                                  | 64.5 ± 0.8             |
| PACD-36-HDI  | 1.14 ± 0.0005                           | 30 ± 7                              | 600 ± 30                                  | 73.8 ± 1.9             |
| PACD-51-IPDI | 1.13 ± 0.0030                           | 30 ± 5                              | 485 ± 17                                  | 69.5 ± 0.5             |

nd – no data

$w_s = 2.6$  and  $2.2\%$  for **TSCD-53-IPDI** and **TSCD-53-HDI**, respectively. This is due to the polymers increased hydrophilicity, a consequence of having the shortest hydrocarbon chain among the examined materials. For PSCD and PACD samples,  $w_s$  values were similar and lower than the tetramethylene derivative ( $1.6$ – $1.9\%$ ). IPDI-based samples have a slightly higher water uptake, which might be influenced by the weaker hydrophobic character of cyclic diisocyanate compared to linear HDI.

#### Analysis of pH of water solutions

The analysis of pH of water solutions in which polymer samples were immersed for 14 and 28 days at  $37^\circ\text{C}$  was performed (Fig. 4B). The average pH values of the tested solutions after either 14 or 28 days were in the range of  $5.1$ – $6.3$

( $\pm 0.016$ ) (Fig. 4B), which was markedly lower than the pH of distilled water prior to the tests ( $\text{pH} = 6.47$ ). Immersion of **TSCD-53-HDI** for 14 or 28 days resulted in pH values of  $5.75$  ( $p < 0.001$ ) and  $5.1$  ( $p < 0.001$ ), respectively. For **TSCD-53-IPDI** immersion values of pH were slightly lower ( $5.6$  and  $5.05$ ), due to the less hydrophobic diisocyanate and increased water uptake. The decrease in pH for TSCD between 14 and 28 days of immersion was the highest. It is possibly due to the accelerating influence of succinic acid, which is a product of hydrolysis. More efficient water penetration leads to increased hydrolysis and, as a consequence of the acidic conditions, acceleration of the process. The pH values of reference distilled water samples after adequate immersion time periods were  $6.35$  and  $6.25$ , respectively. Changes in the pure water pH values could be due to the dissolution of  $\text{CO}_2$  into the air. The pH of **PSCD-44-IPDI** solutions after 14 days and 28 days

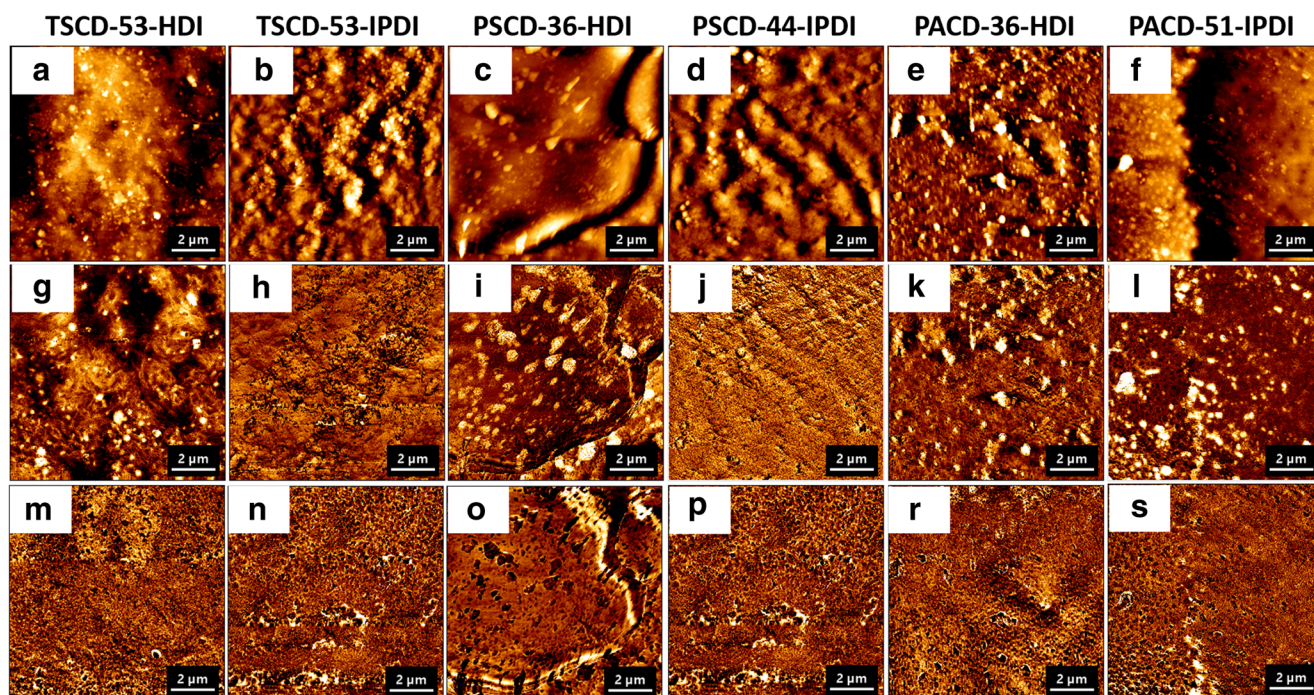


**Fig. 2** Local mechanical properties of poly(ester-carbonate-urea-urethane) surface obtained with atomic force microscopy. Images show quantitative visualization of sample height (A-F), stiffness (G-L) and adhesion (M-S). Scale bar equals  $2\ \mu\text{m}$

**Table 4** Mechanical properties of poly(ester-carbonate-urea-urethane)s surfaces quantified using atomic force microscopy

| Sample       | Stiffness (N/m) | Adhesion (nN) |
|--------------|-----------------|---------------|
| TSCD-53-HDI  | 1.6 ± 0.3       | 14.4 ± 3.9    |
| TSCD-53-IPDI | 2.3 ± 0.2       | 15.2 ± 5.2    |
| PSCD-36-HDI  | 1.2 ± 0.4       | 38.8 ± 15.7   |
| PSCD-44-IPDI | 2.5 ± 0.1       | 20.7 ± 6.2    |
| PACD-36-HDI  | 1.7 ± 0.2       | 14.7 ± 3.5    |
| PACD-51-IPDI | 1.2 ± 0.2       | 11.0 ± 2.9    |

were 5.8 ( $p < 0.05$ ) and 5.3 ( $p < 0.05$ ), respectively. In both time points, no statistical difference was observed for polymers **PSCD-36-HDI** and **PACD-51-IPDI** versus distilled water.

**Evaluation of hemocompatibility**

Before use in medical applications, biomaterials need to meet several important conditions. Thus, the assessment of material safety intended for use in humans is critical. Considering these requirements we have performed several experiments, in which hemocompatibility of tested polymers were investigated. As shown in Fig. 5A, the majority of tested samples had low hemolytic activity after incubation for 24 h. This is particularly important, seeing that a low hemolytic activity for some of the polymers is determined only on the basis of experiments with 4 h incubation times in other studies [40]. However, we also observed that one of our materials (**PACD-51-IPDI**) induced 35% hemolysis.

**Evaluation of cytotoxicity**

Since most of the generated biomaterial scaffolds showed a suitable hemocompatibility, the cytotoxicity was investigated in the next step (Fig. 5B). The polymeric materials were coated with collagen I to enable cellular binding and thus allowing for cellular contact in such a way that indirect cytotoxicity (by

released eluents) and direct cytotoxicity (due to cell-material interaction) could be estimated.

Thus, keratinocytes were seeded on coated biomaterials and cultured for various time points, and the number of attached cells were optically quantified. Calculation of proliferation rate for derivatives with the greatest content of carbonate units (**TSCD-53-HDI** and **TSCD-53-IPDI**) was problematic due to their structure, which makes it unfeasible to take optical images. However, the quantification of cells for most remaining materials revealed an increase in cell number over time for most materials, although the proliferation rate was reduced in comparison to controls (Fig. 5B). Notably, a limited cell growth was observed for **TSCD-53-HDI** and **PSCD-44-IPDI**, indicating decreased cell compatibility. Accordingly, cells cultured on **TSCD-53-HDI** and **PSCD-44-IPDI** showed a small and round morphology, whereas cell cultured on the remaining materials displayed an elongated morphology (Fig. 5C-N).

**Biofilm mass**

Analyses of biofilm mass and AFM-recorded morphology were employed to assess the ability *Candida* cells to colonize the polymeric surfaces (Fig. 6). Compared to the positive control, polystyrene, all tested surfaces had a decreased biofilm mass (Fig. 6A). Furthermore, fungal cell adhesion to surfaces composed of the cyclic form of diisocyanates was lower. Interestingly, in comparison to their linear form, cyclic diisocyanates with pentamethylene succinate or adipate fragments had two to three times lower biofilm mass formation.

The morphology of *Candida tropicalis* biofilm growth on polymeric surfaces is shown in Fig. 6B. It should be noted that there was an increased number of cells present on HDI derivatives of poly(ester-carbonate-urea-urethane)s. This corresponds to the results obtained by biomass quantification. Biofilm formation is also visible on substrates with IPDI derivatives, but cells demonstrate a different growing pattern and morphology. Our results indicate that IPDI derivatives of poly(ester-carbonate-urea-urethane)s possess high anti-biofilm formation properties.

**Fig. 3** Tribological properties of poly(ester-carbonate-urea-urethane)s, where (A) demonstrates coefficient of friction, and (B) mass wear

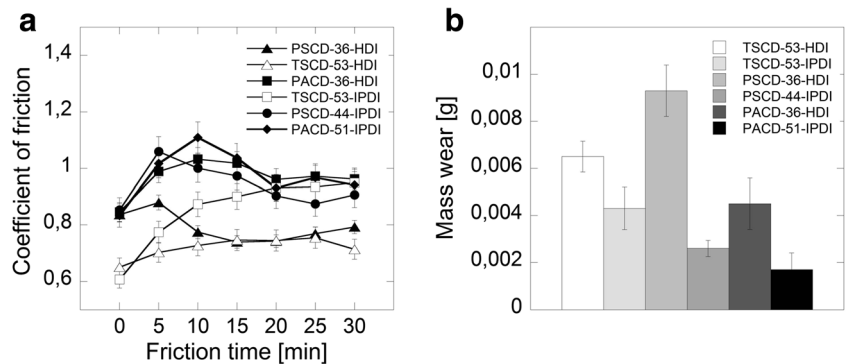
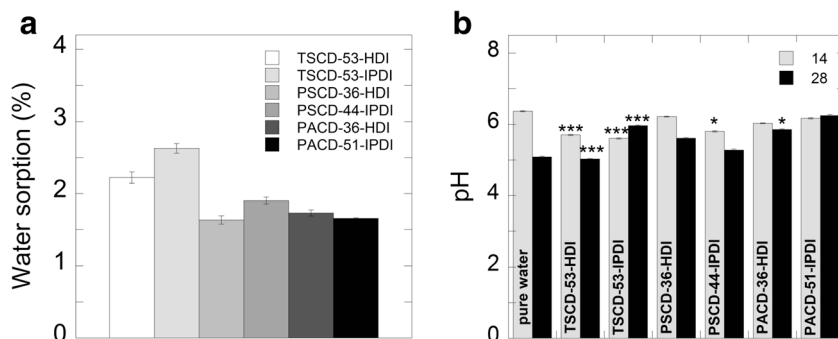


**Fig. 4** Water sorption of samples after 24 h (A) and pH (B) of water solutions, after 14 and 28 days of contact with tested polymers, where: \* $p < 0.05$ , \*\* $p < 0.01$ , \*\*\* $p < 0.001$  vs. pure water



## Discussion

### Mechanical and thermal properties

The main aim of the presented study was to investigate what effect the ester monomer and diisocyanate type (IPDI and HDI) would have on the mechanical and biological properties. DSC studies indicate that introduction of an ester component to the structure of poly(carbonate-urea-urethane)s resulted in decrease of  $T_g$  with simultaneously a small amount of crystalline phase observed [41]. Similar changes of  $T_g$ , in the range of  $-46$  to  $-54$  °C, were described when oligo( $\epsilon$ -caprolactone) diol was mixed with oligo(hexamethylene carbonate) diol and used in poly(ester-carbonate-urethane-urea)s as a soft segments [42].

The mechanical properties of the obtained elastomers are influenced by many factors, such as the number of methylene groups in the diol and the ester derivative structure (Scheme 1 a), the type of diisocyanate (Scheme 1 b), and the content of carbonate/ester groups in the soft segment repeating unit (Table 1). As a result, the final properties are often the sum of competing mechanisms, which complicates elucidation of the relationship between the structure and elastomer properties. The influence of the carbonate groups content in the repeating unit, as well as the type of diisocyanate on thermal and mechanical properties of poly(tetramethylene succinate-co-carbonate-urea-urethane)s were discussed in detail elsewhere [36]. Compared to poly(carbonate-urea-urethane)s obtained in the same manner, but lacking modification with the ester derivative, the samples had much higher elongations at break and higher

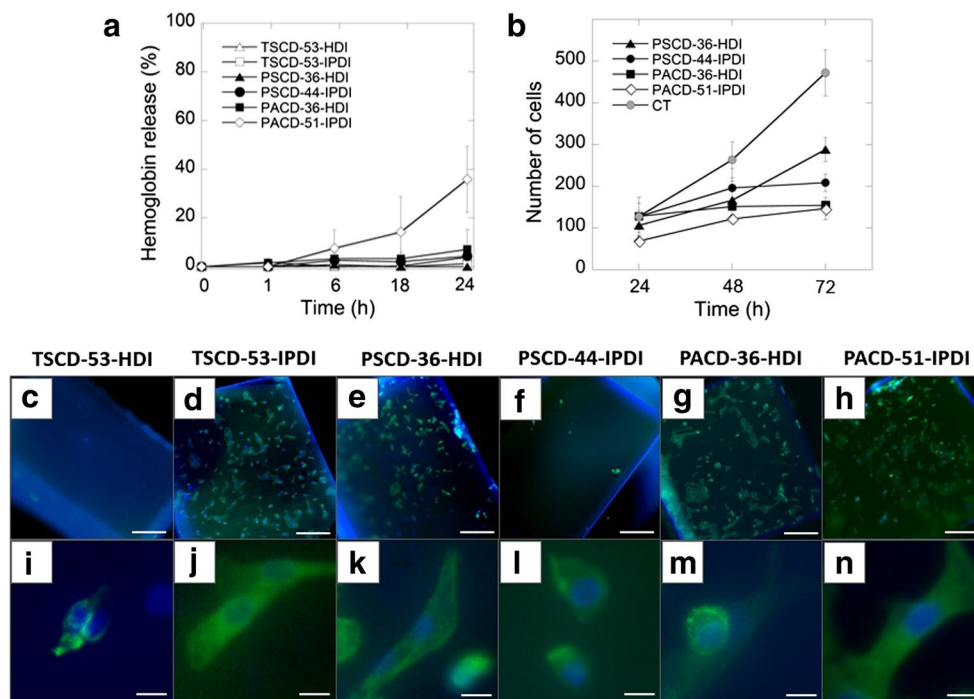


**Fig. 5** Evaluation of cytotoxicity of tested polymers. (A) Hemoglobin release from human red blood cells during 24 h of direct cells contact with tested polymers. (B) Quantitation of keratinocyte cells growing on the surface of selected polymers in comparison to control (CT). Provided cell data equal the number of cells observed in the optical field. Cells were

seeded in the density of  $1.2 \times 10^4$  cells/well. The number of keratinocytes attached to the polymeric surface and morphology of cells is presented in the panels C-N. Scale bar equals 200  $\mu$ m (panels C-D) and 10  $\mu$ m (panels I-N), respectively



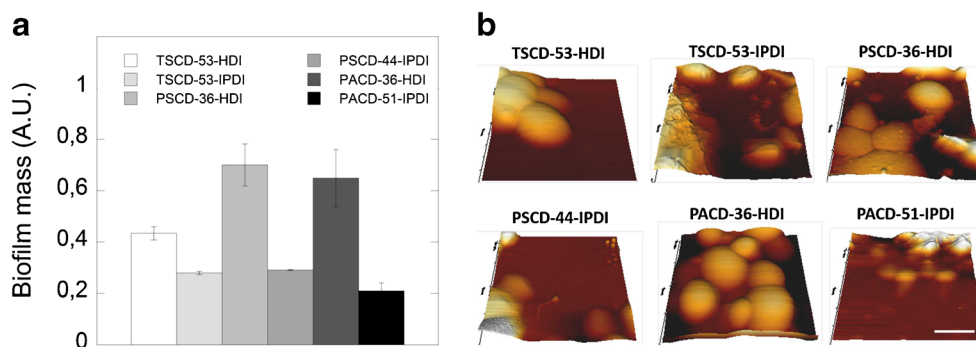


**Fig. 6** *Candida tropicalis* biomass formed on the polymeric surface during 48 h growth time. (A) Formation of biofilm mass on the polyurethane surfaces. (B) 3D height maps of live *Candida tropicalis* growing on

the polymer surfaces: TSCD-53-HDI, TSCD 55-IPDI, PSCD-36-HDI, PSCD-44-IPDI, PACD-36-HDI, and PACD-51-IPDI. Scale bar equals 5  $\mu\text{m}$

hardness simultaneously with similar values of tensile strengths in the range of 20–30 MPa [41]. Poly(ester-urea-urethane)s based on HDI, water, and oligo(1,4-tetramethylene adipate) diol ( $M_n = 1000 \text{ g}\cdot\text{mol}^{-1}$ ), oligo(1,2-dimethylethylene adipate) diol ( $M_n = 800 \text{ g}\cdot\text{mol}^{-1}$ ), and oligo(1,2-dimethylethylene succinate) diol ( $M_n = 710 \text{ g}\cdot\text{mol}^{-1}$ ), have shown tensile strengths of 11.7, 3.0, and 22.7 MPa, respectively [43]. Samples based on oligo( $\delta$ -valerolactone-*co*- $\epsilon$ -caprolactone) diol, BDI and putrescine exhibited similar tensile strength, but much higher elongation at break, around 1300% [44]. In comparison to poly(ester-carbonate-urea-urethane)s described by Hong et al. [42], which were synthesized from oligo( $\epsilon$ -caprolactone) and oligo(1,6-hexamethylene carbonate) diols, tetramethylene diisocyanate, and putrescine, our samples exhibited higher values of tensile strengths and simultaneously were characterized by lower elongation at break.

### Biological properties

Hemolysis testing was able to confirm most materials as hemocompatible due low hemolysis levels. However it also identified **PACD-51-IPDI** as non hemocompatible, rendering this material incompatible as a scaffold in clinical use.

Furthermore, evaluation of cytotoxicity revealed that most polymeric surfaces supported keratinocytes proliferation, although it was lower as compared to polystyrene. Similar effects were observed for high modulus biodegradable polyurethanes synthesized for vascular stents. Sgarioto et al. confirmed that despite the delayed endothelialization of HUVEC on polymers, when compared to tissue-treated culture plates, polymers produced by this research group were highly biocompatible [45]. Thus, it can be concluded that the here tested materials were also compatible with tested cells. Low numbers of attached cells on PACD-51 and TSCD-53 do not indicate cytotoxicity per se, but they might also interfere with cellular binding. Further indirect cellular toxicity testing will be necessary to evaluate the cytotoxicity of these materials.

The restricted biofilm formation on all of the materials but especially on IPDI-based samples indicated them to be

advantageous candidates for implant materials. Such materials have a lower risk of biological contamination during production, packaging and implantation and thus greatly reduce the risk of post-operative infections.

Recent studies indicate that linear polymers synthesized using methyl methacrylate as a backbone monomer and methacrylic and itaconic acids as functional monomers restricted biofilm formation. Cavaleiro et al. suggest that the inhibitory effects were caused by attenuation of quorum sensing through sequestration of signal molecules [46]. Quorum sensing (QS) is a fundamental mechanism responsible for microbial communication and several pathogenic behaviors including virulence factors secretion and biofilm formation. Recently, QS systems have been described for fungal pathogens [47]. Other studies suggest that Nylon-3 polymer (poly- $\beta$ NM) has strong and selective activity against drug-resistant *Candida albicans* in biofilms via inhibition of biofilm formation and by killing of fungal cells in mature biofilms [48]. Additionally, Luiz et al. demonstrated that fraction F2 and subfraction F2.4 of proanthocyanidins polymer-rich fractions obtained from *Stryphnodendronadstringens* strongly reduced biofilm metabolic activity during biofilm formation as well as in mature biofilms. This is unlike fluconazole, which only prevents the biofilm formation [49]. The antifungal activity was confirmed against sessile and dispersion cells, which play a key role in disease progression and display different virulence properties than their planktonic form, including enhanced adherence, biofilm formation, filamentation, and pathogenicity [50].

### Conclusions

Depending on the type of diisocyanate, as well as the ester derivative used, thermal and mechanical properties are varied and can be tailored for application-specific purposes. Samples based on adipic acid derivatives have shown lower glass transition temperature, higher elongation at break and higher tensile strength compared to succinate acid derivative based

PCUUs. Water sorption and changes in pH of the resultant solution after immersion indicate that the samples most prone to water penetration and hydrolysis are those with the most hydrophilic structure, especially obtained with the usage of IPDI. Our aim was to assess clinical applicability as polymeric scaffolds for regenerative medicine, in particular their resistance to biological colonization, i.e. against *Candida* species, their hemocompatibility, and lack of cytotoxicity. It has been shown, that IPDI derived PCUUs exhibit anti-biofilm properties, which make them useful for potential medical applications. In the case of most of the examined samples the hemolysis was in the range of 3% to 10%, which indicates high but variable hemocompatibility. Tested samples were also able to support the growth of human keratinocytes HaCaT on their surfaces when coated with collagen. However, further investigation of the polymer surface structure on the biological properties of potential polymeric scaffolds is needed.

**Acknowledgements** This scientific work was realized in frame of work, no S/WM/1/14 and financed from research funds of Ministry of Science and Higher Education and by the European Union - European Regional Development Fund under Operation Program Innovative Economy – MARGEN (POIG.01.03.01-00-018/08). This study was conducted with the use of equipment purchased by Medical University of Białystok as part of the RPOWP 2007-2013 funding, Priority I, Axis 1.1, contract No. UDA-RPPD.01.01.00-20-001/15-00 dated 26.06.2015.

**Open Access** This article is distributed under the terms of the Creative Commons Attribution 4.0 International License (<http://creativecommons.org/licenses/by/4.0/>), which permits unrestricted use, distribution, and reproduction in any medium, provided you give appropriate credit to the original author(s) and the source, provide a link to the Creative Commons license, and indicate if changes were made.

## References

1. St. John KR (2014) The use of polyurethane materials in the surgery of the spine: a review. *Spine J* 14(12):3038–3047. doi:10.1016/j.spinee.2014.08.012
2. Wang W, Wang C (2012) Polyurethane for biomedical applications: A review of recent developments. In: Davim JP (ed) *The Design and Manufacture of Medical Devices*. 1st edn. Woodhead Publishing, pp 115–151. doi:10.1533/9781908818188.115
3. Greenwood JE, Wagstaff MJD (2016) The use of biodegradable polyurethane in the development of dermal scaffolds. In: Cooper SL, Guan J (eds) *Advances in Polyurethane Biomaterials*. 1st edn. Woodhead Publishing, pp 631–662. doi:10.1016/B978-0-08-100614-6.00022-6
4. Santerre JP, Woodhouse K, Laroche G, Labow RS (2005) Understanding the biodegradation of polyurethanes: from classical implants to tissue engineering materials. *Biomaterials* 26(35):7457–7470. doi:10.1016/j.biomaterials.2005.05.079
5. Król P (2007) Synthesis methods, chemical structures and phase structures of linear polyurethanes. Properties and applications of linear polyurethanes in polyurethane elastomers, copolymers and ionomers. *Prog Mater Sci* 52(6):915–1015. doi:10.1016/j.pmatsci.2006.11.001
6. Hiob MA, Crouch GW, Weiss AS (2016) Elastomers in vascular tissue engineering. *Curr Opin Biotechnol* 40:149–154. doi:10.1016/j.copbio.2016.04.008
7. Zhang X, Battiston KG, McBane JE, Matheson LA, Labow RS, Santerre JP (2016) Design of biodegradable polyurethanes and the interactions of the polymers and their degradation by-products within in vitro and in vivo environments. In: Cooper SL, Guan J (eds) *Advances in Polyurethane Biomaterials*. 1st edn. Woodhead Publishing, pp 75–114. doi:10.1016/B978-0-08-100614-6.00003-2
8. Qu W-Q, Xia Y-R, Jiang L-J, Zhang L-W, Hou Z-S (2016) Synthesis and characterization of a new biodegradable polyurethanes with good mechanical properties. *Chin Chem Lett* 27(1):135–138. doi:10.1016/j.ccllet.2015.07.018
9. Fujimoto KL, Guan J, Oshima H, Sakai T, Wagner WR (2007) In vivo evaluation of a porous, elastic, biodegradable patch for reconstructive cardiac procedures. *Ann Thorac Surg* 83(2):648–654. doi:10.1016/j.athoracsur.2006.06.085
10. Hafeman AE, Zienkiewicz KJ, Zachman AL, Sung H-J, Nanney LB, Davidson JM, Guelcher SA (2011) Characterization of the degradation mechanisms of lysine-derived aliphatic poly(ester urethane) scaffolds. *Biomaterials* 32(2):419–429. doi:10.1016/j.biomaterials.2010.08.108
11. Wang F, Li Z, Lannutti JL, Wagner WR, Guan J (2009) Synthesis, characterization and surface modification of low moduli poly(ether carbonate urethane)ureas for soft tissue engineering. *Acta Biomater* 5(8):2901–2912. doi:10.1016/j.actbio.2009.04.016
12. Roohpour N, Wasikiewicz J, Moshaverinia A, Paul D, Rehman I, Vadgama P (2009) Isopropyl Myristate-modified polyether-urethane coatings as protective barriers for implantable medical devices. *Materials* 2(3):719. doi:10.3390/ma2030719
13. Tanzi MC, Mantovani D, Petrini P, Guidoin R, Laroche G (1997) Chemical stability of polyether urethanes versus polycarbonate urethanes. *J Biomed Mater Res* 36(4):550–559. doi:10.1002/(SICI)1097-4636(19970915)36:4<550::AID-JBM14>3.0.CO;2-E
14. Ionescu M (2005) Polycarbonate Polyols. In: *chemistry and Technology of Polyols for polyurethanes*. Rapra Technology Ltd, Shawbury, pp. 285–294
15. Fernández-d'Arlas B, Alonso-Varona A, Palomares T, Corcuera MA, Eceiza A (2015) Studies on the morphology, properties and biocompatibility of aliphatic diisocyanate-polycarbonate polyurethanes. *Polym Degrad Stab* 122:153–160. doi:10.1016/j.polymdegradstab.2015.10.023
16. Raghunath J, Georgiou G, Armitage D, Nazhat SN, Sales KM, Butler PE, Seifalian AM (2009) Degradation studies on biodegradable nanocomposite based on polycaprolactone/polycarbonate (80:20%) polyhedral oligomeric silsesquioxane. *J Biomed Mater Res A* 91A(3):834–844. doi:10.1002/jbm.a.32335
17. S-h H, Lin Z-C (2004) Biocompatibility and biostability of a series of poly(carbonate)urethanes. *Colloids Surf B Biointerfaces* 36(1):1–12. doi:10.1016/j.colsurfb.2004.04.003
18. Christenson EM, Patel S, Anderson JM, Hiltner A (2006) Enzymatic degradation of poly(ether urethane) and poly(carbonate urethane) by cholesterol esterase. *Biomaterials* 27(21):3920–3926. doi:10.1016/j.biomaterials.2006.03.012
19. Tang YW, Labow RS, Santerre JP (2001) Enzyme-induced biodegradation of polycarbonate-polyurethanes: dependence on hard-segment chemistry. *J Biomed Mater Res* 57(4):597–611. doi:10.1002/1097-4636(20011215)57:4<597::AID-JBM1207>3.0.CO;2-T
20. Labow RS, Meek E, Santerre JP (2001) Hydrolytic degradation of poly(carbonate)-urethanes by monocyte-derived macrophages. *Biomaterials* 22(22):3025–3033. doi:10.1016/S0142-9612(01)00049-7
21. Serkis M, Špírková M, Poreba R, Hodan J, Kredatusová J, Kubies D (2015) Hydrolytic stability of polycarbonate-based polyurethane elastomers tested in physiologically simulated conditions. *Polym*

- Degrad Stab 119:23–34. doi:10.1016/j.polymdegradstab.2015.04.030
22. Seifalian AM, Salacinski HJ, Tiwari A, Edwards A, Bowald S, Hamilton G (2003) In vivo biostability of a poly(carbonate-urea)urethane graft. *Biomaterials* 24(14):2549–2557. doi:10.1016/S0142-9612(02)00608-7
  23. Salacinski HJ, Odlyha M, Hamilton G, Seifalian AM (2002) Thermo-mechanical analysis of a compliant poly(carbonate-urea)urethane after exposure to hydrolytic, oxidative, peroxidative and biological solutions. *Biomaterials* 23(10):2231–2240. doi:10.1016/S0142-9612(01)00356-8
  24. Tang YW, Labow RS, Santerre JP (2001) Enzyme-induced biodegradation of polycarbonate polyurethanes: dependence on hard-segment concentration. *J Biomed Mater Res* 56(4):516–528. doi:10.1002/1097-4636(20010915)56:4<516::AID-JBM1123>3.0.CO;2-B
  25. Kozakiewicz J, Rokicki G, Przybylski J, Sylwestrzak K, Parzuchowski PG, Tomczyk KM (2010) Studies of the hydrolytic stability of poly(urethane-urea) elastomers synthesized from oligocarbonate diols. *Polym Degrad Stab* 95(12):2413–2420. doi:10.1016/j.polymdegradstab.2010.08.017
  26. Chen W, Meng F, Cheng R, Deng C, Feijen J, Zhong Z (2014) Advanced drug and gene delivery systems based on functional biodegradable polycarbonates and copolymers. *J Control Release* 190:398–414. doi:10.1016/j.jconrel.2014.05.023
  27. Khan I, Smith N, Jones E, Finch DS, Cameron RE (2005) Analysis and evaluation of a biomedical polycarbonate urethane tested in an in vitro study and an ovine arthroplasty model. Part I: materials selection and evaluation. *Biomaterials* 26(6):621–631. doi:10.1016/j.biomaterials.2004.02.065
  28. Khan I, Smith N, Jones E, Finch DS, Cameron RE (2005) Analysis and evaluation of a biomedical polycarbonate urethane tested in an in vitro study and an ovine arthroplasty model. Part II: in vivo investigation. *Biomaterials* 26(6):633–643. doi:10.1016/j.biomaterials.2004.02.064
  29. Cipriani E, Bracco P, Kurtz SM, Costa L, Zanetti M (2013) In-vivo degradation of poly(carbonate-urethane) based spine implants. *Polym Degrad Stab* 98(6):1225–1235. doi:10.1016/j.polymdegradstab.2013.03.005
  30. Vrancken ACT, Buma P, van Tienen TG (2013) Synthetic meniscus replacement: a review. *Int Orthop* 37(2):291–299. doi:10.1007/s00264-012-1682-7
  31. Elsner JJ, Mezape Y, Hakshur K, Shemesh M, Linder-Ganz E, Shterling A, Eliaz N (2010) Wear rate evaluation of a novel polycarbonate-urethane cushion form bearing for artificial hip joints. *Acta Biomater* 6(12):4698–4707. doi:10.1016/j.actbio.2010.07.011
  32. Guegan S, Lanternier F, Rouzaud C, Dupin N, Lortholary O (2016) Fungal skin and soft tissue infections. *Curr Opin Infect Dis* 29(2):124–130. doi:10.1097/qco.0000000000000252
  33. Hasan F, Xess I, Wang X, Jain N, Fries BC (2009) Biofilm formation in clinical *Candida* isolates and its association with virulence. *Microbes Infect* 11(8–9):753–761. doi:10.1016/j.micinf.2009.04.018
  34. Sherry L, Rajendran R, Lappin DF, Borghi E, Perdoni F, Falleni M, Tosi D, Smith K, Williams C, Jones B, Nile CJ, Ramage G (2014) Biofilms formed by *Candida Albicans* bloodstream isolates display phenotypic and transcriptional heterogeneity that are associated with resistance and pathogenicity. *BMC Microbiol* 14:182. doi:10.1186/1471-2180-14-182
  35. Sardi JC, Scorzoni L, Bernardi T, Fusco-Almeida AM, Mendes Giannini MJ (2013) *Candida* species: current epidemiology, pathogenicity, biofilm formation, natural antifungal products and new therapeutic options. *J Med Microbiol* 62(Pt 1):10–24. doi:10.1099/jmm.0.045054-0
  36. Mazurek MM, Rokicki G (2013) Investigations on the synthesis and properties of biodegradable poly(ester-carbonate-urea-urethane)s. *Pol J Chem Technol* 15(4):80–88. doi:10.2478/pjct-2013-0073
  37. Tomczyk K, Parzuchowski P, Kozakiewicz J, Przybylski J, Rokicki G (2010) Synthesis of oligocarbonate diols from a “green monomer” – dimethyl carbonate – as soft segments for poly(urethane-urea) elastomers. *Polimery* 5:366–372
  38. Mystkowska J, Jałbrzykowski M, Dąbrowski JR (2013) Tribological properties of selected self-made solutions of synthetic saliva. *Solid State Phenom* 199:567–572. doi:10.4028/www.scientific.net/SSP.199.567
  39. Elsner JJ, Shemesh M, Shefy-Peleg A, Gabet Y, Zylberberg E, Linder-Ganz E (2015) Quantification of in vitro wear of a synthetic meniscus implant using gravimetric and micro-CT measurements. *J Mech Behav Biomed Mater* 49:310–320. doi:10.1016/j.jmbbm.2015.05.017
  40. Faria M, Geraldes V, de Pinho MN (2012) Surface characterization of asymmetric bi-soft segment poly(ester urethane urea) membranes for blood-oxygenation medical devices. *Int J Biomater* 2012:9. doi:10.1155/2012/376321
  41. Mazurek MM, Tomczyk K, Auguścik M, Ryszkowska J, Rokicki G (2015) Influence of the soft segment length on the properties of water-cured poly(carbonate-urethane-urea)s. *Polym Adv Technol* 26(1):57–67. doi:10.1002/pat.3419
  42. Hong Y, Guan J, Fujimoto KL, Hashizume R, Pelinescu AL, Wagner WR (2010) Tailoring the degradation kinetics of poly(ester carbonate urethane)urea thermoplastic elastomers for tissue engineering scaffolds. *Biomaterials* 31(15):4249–4258. doi:10.1016/j.biomaterials.2010.02.005
  43. Tang D, Noordover BAJ, Sablong RJ, Koning CE (2012) Thermoplastic poly(urethane urea)s from novel, bio-based amorphous polyester Diols. *Macromol Chem Phys* 213(23):2541–2549. doi:10.1002/macp.201200397
  44. Ma Z, Hong Y, Nelson DM, Pichamuthu JE, Leeson CE, Wagner WR (2011) Biodegradable polyurethane ureas with variable polyester or polycarbonate soft segments: effects of crystallinity, molecular weight, and composition on mechanical properties. *Biomacromolecules* 12(9):3265–3274. doi:10.1021/bm2007218
  45. Sgarioto M, Adhikari R, Gunatillake PA, Moore T, Patterson J, Nagel M-D, Malherbe F (2015) High modulus biodegradable polyurethanes for vascular stents: evaluation of accelerated in vitro degradation and cell viability of degradation products. *Front Bioeng Biotechnol* 3:52. doi:10.3389/fbioe.2015.00052
  46. Cavaleiro E, Duarte AS, Esteves AC, Correia A, Whitcombe MJ, Piletska EV, Piletsky SA, Chianella I (2015) Novel linear polymers able to inhibit bacterial quorum sensing. *Macromol Biosci* 15(5):647–656. doi:10.1002/mabi.201400447
  47. Albuquerque P, Casadevall A (2012) Quorum sensing in fungi - a review. *Med Mycol* 50(4):337–345. doi:10.3109/13693786.2011.652201
  48. Liu R, Chen X, Falk SP, Masters KS, Weisblum B, Gellman SH (2015) Nylon-3 polymers active against drug-resistant *Candida Albicans* biofilms. *J Am Chem Soc* 137(6):2183–2186. doi:10.1021/ja512567y
  49. Luiz RL, Vila TV, de Mello JC, Nakamura CV, Rozental S, Ishida K (2015) Proanthocyanidins polymeric tannin from *Stryphnodendron Adstringens* are active against *Candida Albicans* biofilms. *BMC Complement Altern Med* 15:68. doi:10.1186/s12906-015-0597-4
  50. Uppuluri P, Chaturvedi AK, Srinivasan A, Banerjee M, Ramasubramaniam AK, Kohler JR, Kadosh D, Lopez-Ribot JL (2010) Dispersion as an important step in the *Candida Albicans* biofilm developmental cycle. *PLoS Pathog* 6(3):e1000828. doi:10.1371/journal.ppat.1000828